Analysis of reciprocity of cos-Gaussian and cosh-Gaussian laser beams in a turbulent atmosphere

Halil Tanyer Eyyuboğlu

Department of Electronic and Communication Engineering, Çankaya University, Öğretmenler Cad. No. 14 Yüzüncüyıl, 06530 Balgat, Ankara, Turkey
h.eyyuboglu@cankaya.edu.tr

Yahya Baykal

Department of Electronic and Communication Engineering, Çankaya University, Öğretmenler Cad. No. 14 Yüzüncüyıl, 06530 Balgat, Ankara, Turkey
y.baykal@cankaya.edu.tr

Abstract: In a turbulent atmosphere, starting with a cos-Gaussian excitation at the source plane, the average intensity profile at the receiver plane is formulated. This average intensity profile is evaluated against the variations of link lengths, turbulence levels, two frequently used free-space optics wavelengths, and beam displacement parameters. We show that a cos-Gaussian beam, following a natural diffraction, is eventually transformed into a cosh-Gaussian beam. Combining our earlier results with the current findings, we conclude that cos-Gaussian and cosh-Gaussian beams act in a reciprocal manner after propagation in turbulence. The rates (paces) of conversion in the two directions are not the same. Although the conversion of cos-Gaussian beams to cosh-Gaussian beams can happen over a wide range of turbulence levels (low to moderate to high), the conversion of cosh-Gaussian beams to cos-Gaussian beams is pronounced under relatively stronger turbulence conditions. Source and propagation parameters that affect this reciprocity have been analyzed.

OCIS codes: (010.1330) Atmospheric turbulence, (010.1300) Atmospheric propagation, (010.3310) Laser beam transmission, (010.1290) Atmospheric optics.

References and links

1. A. A. Tovar and L. W. Casperson, "Production and propagation of Hermite sinusoidal-Gaussian laser beams," J. Opt. Soc. Am. A **15**, 2425–2432 (1998).
2. L. W. Casperson and A. A. Tovar, "Hermite sinusoidal-Gaussian beams in complex optical systems," J. Opt. Soc. Am. A **15**, 954–961 (1998).
3. B. Lü, H. Ma, and B. Zhang, "Propagation properties of cosh-Gaussian beams," Opt. Commun. **164**, 165–170 (1999).
4. D. Zhao, H. Mao, and H. Liu, "Propagation of off-axial Hermite-cosh-Gaussian laser beams," J. Opt. A **6**, 77–83 (2004).
5. S. Yu, H. Guo, X. Fu, and W. Hu, "Propagation properties of elegant Hermite-cosh-Gaussian laser beams," Opt. Commun. **204**, 59–66 (2002).
6. S. Konar and J. Soumendu, "Linear and nonlinear propagation of sinh-Gaussian pulses in dispersive media possessing Kerr nonlinearity," Opt. Commun. **236**, 7–20 (2004).
7. N. Zhou and G. Zeng, "Propagation properties of Hermite-cosine-Gaussian beams through a paraxial optical *ABCD* system with hard-edge aperture," Opt. Commun. **232**, 49–59 (2004).
8. Y. Song. G. Wangyi, and G. Hong, "Optical resonator with hyperbolic-cosine-Gaussian modes," Opt. Commun. **221**, 241–247 (2003).
9. Z. I. Feizulin and Y. Kravtsov, "Broadening of a laser beam in a turbulent medium," Radiophys. Quantum Electron. **10**, 33–35 (1967).
10. A. I. Kon and V. I. Tatarskii, "On the theory of propagation of partially coherent light beams in a turbulent atmosphere," Radiophys. Quantum Electron. **15**, 1187–1192 (1972).
11. M. S. Belen'kii, A. I. Kon, and V. L. Mironov, "Turbulent distortions of the spatial coherence of a laser beam," Sov. J. Quantum Electron. **7**, 287–290 (1977).

#4763 - $15.00 US Received 7 July 2004; revised 15 August 2004; accepted 13 September 2004

12. S. C. H. Wang and M. A. Plonus, "Optical beam propagation for a partially coherent source in the turbulent atmosphere," J. Opt. Soc. Am. **69**, 1297–1304 (1979).
13. M. S. Belen'kii and V. L. Mironov, "Phase fluctuations of a multimode laser field in a turbulent atmosphere," Sov. J. Quantum Electron. **12**, 3–6 (1982).
14. C. Y. Young, Y. V. Gilchrest, and B. R. Macon, "Turbulence induced beam spreading of higher order mode optical waves," Opt. Eng. **41**, 1097–1103 (2002).
15. Y. Baykal, "The correlation and structure functions of Hermite-sinusoidal-Gaussian laser beams in a turbulent atmosphere," J. Opt. Soc. Am. A **21**, 1290–1299 (2004).
16. H. T. Eyyuboğlu and Y. Baykal, "Average intensity and spreading of cosh-Gaussian laser beams in the turbulent atmosphere,"Applied Optics, submitted for publication.
17. A. Ishimaru, "Phase fluctuations in a turbulent medium," Applied Optics **16**, 3190-3192 (1977).
18. I. S. Gradysteyn, and I. M. Ryzhik, *Tables of Integrals, Series and Products* (Academic Press, New York, 1980).

1. Introduction

Production and propagation in free space (i.e., in the absence of turbulence) of general Hermite-sinusoidal-Gaussian (HSG) laser beams are studied [1] and applied to complex optical systems.[2] HSG beams cover a broad range of special cases of beams such as cosh-Gaussian and cos-Gaussian types. One of the easiest methods for the generation of such special cases is to use an ordinary Gaussian beam as an incident beam on an appropriate transmission or reflection aperture. If a cosh-Gaussian beam is to be generated, a Gaussian beam is made incident on an aperture that has a cosh-Gaussian transmission function. These beams are used in applications for which efficient extraction of energy is required. For example, cosh-Gaussian dependence exhibits a concentration of energy in the outer lobes of a beam that can be used in the space diversity applications in free-space optic (FSO) systems. Also, considerable studies are being made to search for applications of HSG beams by use of *ABCD* optical systems. Propagation in free space of special cases of HSG beams such as cosh-Gaussian beams,[3] off-axial Hermite-cosh-Gaussian beams,[4] elegant Hermite-cosh-Gaussian beams,[5] and sinh-Gaussian pulses[6] are investigated. Hermite-cos-Gaussian beams that pass through a paraxial optical *ABCD* system with a hard-edge aperture are also examined.[7] An optical resonator with cosh-Gaussian modes is presented.[8] In the presence of atmospheric turbulence, second-order effects exist for Gaussian,[9–12] multimode,[13] and higher-order beams.[14] The correlation and structure functions of HSG laser beams in a turbulent atmosphere were recently formulated,[15] and we found the average intensity and spreading of cosh-Gaussian laser beams in atmospheric turbulence.[16]

Atmospheric turbulence plays a significant role in the performance of FSO links that have become competitive in the broadband access networks in recent years. In general, we are interested in investigating the effect of turbulence when different forms of excitation are used. Our main motivation is to understand whether the use of some special form of HSG laser beams in FSO access communication systems will improve system performance. The first step is to determine the received intensity profile that will affect the receiver design. We are also studying the fourth-order effects of HSG beams such as scintillation, but here we report only the second-order results. Specifically we are concerned with determining how the average intensity profile of a cos-Gaussian beam is altered during propagation in practical FSO links. For this purpose, the source plane excitation is described by a cos-Gaussian laser beam. We derived the average intensity profile of this beam at the receiver plane after it has passed through a turbulent atmosphere.

The limiting cases of our formulation are compared with the known Gaussian beam wave solution in the turbulent atmosphere and cos-Gaussian beam solution in free space (i.e., in the absence of turbulence), and we found that there is exact conformity to these limiting cases.

Numerical evaluations are made at various link lengths, turbulence levels, beam displacement parameters, and at the most frequently used FSO wavelengths of 0.85 and 1.55 μm. We observed that a cos-Gaussian beam, following the natural diffraction, is eventually transformed into a cosh-Gaussian beam. We recently formulated[16] the average received

#4763 - $15.00 US Received 7 July 2004; revised 15 August 2004; accepted 13 September 2004

intensity profile and the spreading of cosh-Gaussian laser beams in a turbulent medium. Combining our earlier results[16] with the present findings, we conclude that cos-Gaussian and cosh-Gaussian beams act in a reciprocal manner after propagation in turbulence. Source and propagation parameters that affect this reciprocity have been analyzed.

2. Propagation of a cos-Gaussian beam in a turbulent atmosphere

Figure 1 supplies the propagation geometry. The source plane is located at the coordinate $(\boldsymbol{s}, z = 0)$, location $(\boldsymbol{p}, z = L)$ refers to the receiver plane, z is the propagation axis, and L is the link length. The sets $\boldsymbol{s} = (s_x, s_y)$ and $\boldsymbol{p} = (p_x, p_y)$ are the transverse source and receiver coordinates, respectively.

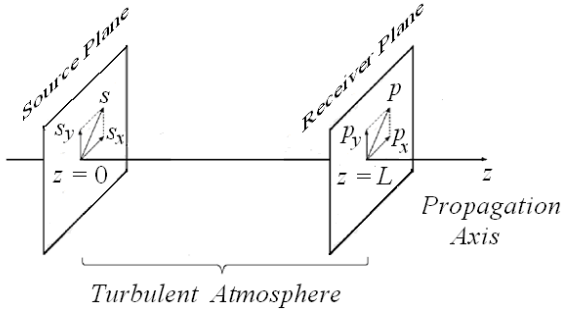

Fig. 1. Propagation geometry.

The sinusoidal-Gaussian beam wave field at the source plane $(z = 0)$, which is essentially a Gaussian beam with complex displacement parameters of $V_x = V_{xr} + iV_{xi}$, $Y_x = Y_{xr} + iY_{xi}$ along the s_x direction and $V_y = V_{yr} + iV_{yi}$, $Y_y = Y_{yr} + iY_{yi}$ along the s_y direction, is written as

$$u_s(s_x, s_y, z = 0) = 0.5A\exp(-i\phi)\exp\left[-0.5\left(s_x^2/\alpha_{sx}^2 + s_y^2/\alpha_{sy}^2\right)\right] \times\left\{\exp\left[i(V_x s_x + V_y s_y)\right] + \exp\left[i(Y_x s_x + Y_y s_y)\right]\right\} \quad (1)$$

where A is the amplitude of the field at the origin of the source plane (i.e., at $s_x = s_y = z = 0$); ϕ is the constant phase factor, $i = (-1)^{1/2}$; α_{sx} and α_{sy} are the respective source sizes of the Gaussian beam in the s_x and s_y directions; V_{xr}, V_{xi} denote the real and imaginary components of V_x; and V_{yr}, V_{yi} denote the real and imaginary components of V_y. Likewise, Y_{xr}, Y_{xi} are the real and imaginary components of Y_x, whereas Y_{yr}, Y_{yi} refer to the real and imaginary components of Y_y. Here, focal lengths along both s_x and s_y are taken to be infinite.

A cos-Gaussian laser beam is generated by choosing $V_x = -Y_x = -V_{xr}$ and $V_y = -Y_y = -V_{yr}$. Similarly, one can obtain a cosh-Gaussian laser beam by setting $V_x = -Y_x = iV_{xi}$ and $V_y = -Y_y = iV_{yi}$. Thus, use of Eq. (1) with $A = 1$, the intensity distribution of the cos-Gaussian beam at the exit plane of the laser is

#4763 - $15.00 US Received 7 July 2004; revised 15 August 2004; accepted 13 September 2004

$$I_s(s_x, s_y, z=0) = \exp\left[-\left(s_x^2/\alpha_{sx}^2 + s_y^2/\alpha_{sy}^2\right)\right]\cos^2\left(V_{xr}s_x + V_{yr}s_y\right) \tag{2}$$

At the receiver plane $(z = L)$, we represented field $u(\boldsymbol{p}, L, t)$ by applying the Huygens–Fresnel principle as follows:

$$u(\boldsymbol{p}, L, t) = k\exp(ikL)/(2\pi iL)\int_{-\infty}^{\infty}\int_{-\infty}^{\infty}\boldsymbol{d}^2\boldsymbol{s}\, u_s(\boldsymbol{s}) \\ \times \exp\left[ik(\boldsymbol{p}-\boldsymbol{s})^2/(2L) + \psi(\boldsymbol{s}, \boldsymbol{p}) - i2\pi ft\right] \tag{3}$$

where k is the wave number; $u_s(\boldsymbol{s})$ is the field of a cos-Gaussian beam at the source plane $(z = 0)$ as provided by Eq. (1); $\psi(\boldsymbol{s}, \boldsymbol{p})$ is the solution to the Rytov method that represents the random part of the complex phase of a spherical wave that propagates from the source point $(\boldsymbol{s}, z = 0)$ to the receiver point $(\boldsymbol{p}, z = L)$; f is the frequency; and t denotes time.

The average intensity at the receiver plane is $<I(\boldsymbol{p}, L)> = <u(\boldsymbol{p}, L, t)u^*(\boldsymbol{p}, L, t)>$ where the * represents the complex conjugate and the $< >$ indicate the ensemble average over the medium statistics covering the log-amplitude and phase fluctuations due to the atmospheric turbulence. With this definition, Eq. (3) is transformed into

$$<I(\boldsymbol{p}, L)> = k^2/(2\pi L)^2\int_{-\infty}^{\infty}\int_{-\infty}^{\infty}\int_{-\infty}^{\infty}\int_{-\infty}^{\infty}\boldsymbol{d}^2\boldsymbol{s}_1\boldsymbol{d}^2\boldsymbol{s}_2 u_s(\boldsymbol{s}_1)u_s^*(\boldsymbol{s}_2)\exp\left\{ik\left[(\boldsymbol{p}-\boldsymbol{s}_1)^2 - (\boldsymbol{p}-\boldsymbol{s}_2)^2\right]/(2L)\right\} \\ \times <\exp\left[\psi(\boldsymbol{s}_1, \boldsymbol{p}) + \psi^*(\boldsymbol{s}_2, \boldsymbol{p})\right]> \tag{4}$$

The ensemble average term within the integrand of Eq. (4) is [12]

$$<\exp\left[\psi(\boldsymbol{s}_1, \boldsymbol{p}) + \psi^*(\boldsymbol{s}_2, \boldsymbol{p})\right]> = \exp\left[-0.5D_\psi(\boldsymbol{s}_1 - \boldsymbol{s}_2)\right] = \exp\left[-\rho_0^{-2}(\boldsymbol{s}_1 - \boldsymbol{s}_2)^2\right] \tag{5}$$

where $D_\psi(\boldsymbol{s}_1 - \boldsymbol{s}_2)$ is the wave structure function, and $\rho_0 = \left(0.545\, C_n^2 k^2 L\right)^{-3/5}$ is the coherence length of a spherical wave that propagates in the turbulent medium, with C_n^2 being the constant of the structure. Here we state that the Rytov method is known to be valid in weak turbulence, especially when fourth-order moments such as scintillations are considered. Customarily, weak turbulence is associated with Rytov log amplitude variance $0.307C_n^2k^{7/6}L^{11/6}$, which is quite smaller than unity. However, here we study the second-order moment by utilizing the wave structure function that is approximated by the phase structure function. Rytov's phase structure function usually accepted to be valid not only for the case of "weak fluctuations", but for the case of "strong fluctuations" as well [17], i.e., when $0.307C_n^2k^{7/6}L^{11/6} > 0.5$. For completeness and clarity, we note that in order to obtain simpler and viewable analytical results, we have also employed a quadratic approximation [12] for the Rytov's phase structure function.

#4763 - $15.00 US Received 7 July 2004; revised 15 August 2004; accepted 13 September 2004

Substituting Eqs. (1) and (5) into Eq. (4) and expanding the transverse source and transverse receiver coordinates into their corresponding x and y components, the average intensity at the receiver plane becomes

$$
\begin{aligned}
<I(\boldsymbol{p},L)> = 0.25k^2/(2\pi L)^2 \int_{-\infty}^{\infty}\int_{-\infty}^{\infty}\int_{-\infty}^{\infty}\int_{-\infty}^{\infty} ds_{1x}\,ds_{1y}\,ds_{2x}\,ds_{2y}\,\exp\left[-0.5\left(s_{1x}^2+s_{2x}^2\right)/\alpha_{sx}^2-0.5\left(s_{1y}^2+s_{2y}^2\right)/\alpha_{sy}^2\right] \\
\times \left\{\exp\left[iV_{xr}\left(s_{1x}+s_{2x}\right)+iV_{yr}\left(s_{1y}+s_{2y}\right)\right]+\exp\left[-iV_{xr}\left(s_{1x}+s_{2x}\right)-iV_{yr}\left(s_{1y}+s_{2y}\right)\right]\right. \\
\left.+\ \exp\left[iV_{xr}\left(s_{1x}-s_{2x}\right)+iV_{yr}\left(s_{1y}-s_{2y}\right)\right]+\exp\left[-iV_{xr}\left(s_{1x}-s_{2x}\right)-iV_{yr}\left(s_{1y}-s_{2y}\right)\right]\right\} \\
\times \exp\left[0.5(ik/L)\left(s_{1x}^2-2p_x s_{1x}-s_{2x}^2+2p_x s_{2x}+s_{1y}^2-2p_y s_{1y}-s_{2y}^2+2p_y s_{2y}\right)\right] \\
\times \exp\left[-\rho_0^{-2}\left(s_{1x}^2-2s_{1x}s_{2x}+s_{2x}^2+s_{1y}^2-2s_{1y}s_{2y}+s_{2y}^2\right)\right] \qquad (6)
\end{aligned}
$$

By following the steps outlined in Appendix A, the average intensity at the receiver plane is

$$
\begin{aligned}
<I(\boldsymbol{p},L)> = 0.5(k/L)^2\,\rho_0^4\,(D_{sx}D_{sy})^{-1/2}\exp\left\{-\left(\rho_0^4k^2/L^2\right)\left[p_x^2/\left(\alpha_{sx}^2D_{sx}\right)+p_y^2/\left(\alpha_{sy}^2D_{sy}\right)\right]\right\} \\
\times\left(\exp\left\{-2\rho_0^2\left[V_{xr}^2\left(\rho_0^2+4\alpha_{sx}^2\right)/\left(\alpha_{sx}^2D_{sx}\right)+V_{yr}^2\left(\rho_0^2+4\alpha_{sy}^2\right)/\left(\alpha_{sy}^2D_{sy}\right)\right]\right\}\right. \\
\times\ \cos\left[\left(2\rho_0^4k^2/L^2\right)\left(V_{xr}p_x/D_{sx}+V_{yr}p_y/D_{sy}\right)\right] \\
+\exp\left\{-\rho_0^4\left[V_{xr}^2/\left(\alpha_{sx}^2D_{sx}\right)+V_{yr}^2/\left(\alpha_{sy}^2D_{sy}\right)\right]\right\} \\
\left.\times\cosh\left\{\left(2\rho_0^4k/L\right)\left[V_{xr}p_x/\left(\alpha_{sx}^2D_{sx}\right)+V_{yr}p_y/\left(\alpha_{sy}^2D_{sy}\right)\right]\right\}\right) \qquad (7)
\end{aligned}
$$

where the parameters that appear in Eq. (7) are thoroughly defined in Appendix A. Because of the nature of Eq. (7), the average intensity profile of the receiver plane is initially cos, but source and propagation parameters eventually force it to change to a cosh type. To consider the conditions under which this happens, we compare the cos and cosh terms that include the accompanying exponential factors. Since for all cases of interest $\alpha_{sx} > V_{xr}^{-1}$ and/or $\alpha_{sy} > V_{yr}^{-1}$, the cos term becomes quite negligible when $k\alpha_{sx}^2/L <\sim 1$, $k\alpha_{sy}^2/L <\sim 1$ and $\alpha_{sx} >\sim \rho_0$, $\alpha_{sy} >\sim \rho_0$.

3. Limiting cases

Here Eq. (7) is checked and was determined to reduce to the following limiting cases correctly. Here we note that, although Eq. (7) is considered in the following several limiting cases for which there are already some available results, this kind of testing might be necessary but not sufficient to prove the accuracy of our formulation. We should establish this accuracy by comparing our numerical results with the experimental work. However, to our knowledge no experimental work exists in the literature to compare and validate Eq. (7) for all cases.

3.1. The average intensity distribution at the receiver plane defined by Eq. (7) is evaluated at zero link length, i.e., for $L = 0$. Within this limit, Eq. (7) was found to reduce to the intensity at the source plane as expressed by Eq. (2). In approaching the source plane p_x and p_y should consecutively be replaced by s_x and s_y.

#4763 - $15.00 US Received 7 July 2004; revised 15 August 2004; accepted 13 September 2004

3.2. To determine the limit of a Gaussian beam in free space, we evaluated Eq. (7) with $C_n^2 = 0$ (or alternatively $\rho_0 \to \infty$) and $V_{xr} = V_{yr} = 0$. A symmetrical beam was taken by choosing $\alpha_{sx} = \alpha_{sy} = \alpha_s$. Then the average intensity in Eq. (7) simplified to

$$I(\boldsymbol{p}, L) = \left[k^2\alpha_s^4 / \left(L^2 + k^2\alpha_s^4\right)\right] \exp\left\{-\left[k^2\alpha_s^2 / \left(L^2 + k^2\alpha_s^4\right)\right]\left(p_x^2 + p_y^2\right)\right\} \tag{8}$$

Equation (8) matches the free-space propagation limit examined in Ref. 14. The precise correspondence of Eq. (8) in this paper with Eq. (5) of Ref. 14 is accomplished by noting that $k^2\alpha_s^2 / \left(L^2 + k^2\alpha_s^4\right) = 2/W^2$, $2^{0.5}\alpha_s = W_0$, $p_x = x$, and $p_y = y$.

3.3. Next, our formula in Eq. (7) is checked against the existing result of a Gaussian beam in turbulence. To achieve this, we selected $V_{xr} = V_{yr} = 0$ and also constituted symmetry in the *x* and *y* directions so that $\alpha_{sx} = \alpha_{sy} = \alpha_s$. With these conditions, Eq. (7) becomes

$$< I(\boldsymbol{p}, L) >= \left[k^2\alpha_s^4\rho_0^2 / \left(\rho_0^2L^2 + 4\alpha_s^2L^2 + k^2\alpha_s^4\rho_0^2\right)\right] \exp\left[-k^2\alpha_s^2\rho_0^2\left(p_x^2 + p_x^2\right) / \left(\rho_0^2L^2 + 4\alpha_s^2L^2 + k^2\alpha_s^4\rho_0^2\right)\right] \tag{9}$$

Equation (9) agrees with Eq. (12) of Ref. 12. To establish this agreement, we adapted the parameters in Eq. (12) of Ref. [12] as

$p_d = 0$, $p_c^2 = p_x^2 + p_y^2$, $F = \infty$, $\zeta = 0$, $A_0 = 1$, and $\alpha_o = \alpha_s$.

3.4. Here we compare our results with the cos-Gaussian beam formulation in free space (in the absence of turbulence). For this purpose, we set $C_n^2 = 0$, thus the average intensity in Eq. (7) leads to

$$I(\boldsymbol{p}, L) = 0.5k^2\alpha_{sx}^2\alpha_{sy}^2 g_x^{0.5} g_y^{0.5} \exp\left\{-k^2\left[\alpha_{sx}^2 g_x p_x^2 + \alpha_{sy}^2 g_y p_y^2\right]\right\} \exp\left\{-L^2\left[\alpha_{sx}^2 V_{xr}^2 g_x + \alpha_{sy}^2 V_{yr}^2 g_y\right]\right\}$$

$$\times\left(\cos\left\{2k^2\left[\alpha_{sx}^4 V_{xr} g_x p_x + \alpha_{sy}^4 V_{yr} g_y p_y\right]\right\} + \cosh\left\{2kL\left[\alpha_{sx}^2 V_{xr} g_x p_x + \alpha_{sy}^2 V_{yr} g_y p_y\right]\right\}\right) \tag{10}$$

where $g_x = \left(L^2 + k^2\alpha_{sx}^4\right)^{-1}$ and $g_y = \left(L^2 + k^2\alpha_{sy}^4\right)^{-1}$. After reverting to a single coordinate system in the sense that $\alpha_{sx} = \alpha_{sy} = w_o / 2^{0.5}$, $p_x = p_y = x / 2^{0.5}$, $V_{xr} = V_{yr} = \Omega_o / 2^{0.5}$, Eq. (10) becomes identical to the intensity equivalent of the field expression of Eq. (14) in Ref. 7 (when the free-space unapertured option is chosen).

3.5. Here we consider the average intensity distribution at the receiver plane as given in Eq. (7) with the limit of L being too large, i.e., $L \to \infty$. In this case, since the argument of the cosh term is proportional to $1/L$, it becomes the dominating part, hence the entire cos term, together with its accompanying exponential, virtually drop out of the equation. In this limit Eq. (7) scales down to

#4763 - $15.00 US Received 7 July 2004; revised 15 August 2004; accepted 13 September 2004

$$< I\left(\boldsymbol{p}, L \to \infty\right) >= 0.5\left(k/L\right)^2 \rho_0^4 (D_{sx} D_{sy})^{-1/2} \exp\left\{-\left(\rho_0^4 k^2 / L^2\right)\left[\, p_x^2 / \left(\alpha_{sx}^2 D_{sx}\right) + p_y^2 / \left(\alpha_{sy}^2 D_{sy}\right)\right]\right\}$$
$$\times \exp\left\{-\rho_0^4 \left[V_{xr}^2 / \left(\alpha_{sx}^2 D_{sx}\right) + V_{yr}^2 / \left(\alpha_{sy}^2 D_{sy}\right)\right]\right\}$$
$$\times \cosh\left\{\left(2\rho_0^4 k / L\right)\left[V_{xr} p_x / \left(\alpha_{sx}^2 D_{sx}\right) + V_{yr} p_y / \left(\alpha_{sy}^2 D_{sy}\right)\right]\right\} \qquad (11)$$

By taking $\partial / \partial p_x$ and $\partial / \partial p_y$ of Eq. (11) and setting them independently to zero, we found the peak locations to be fixed at $p_{xp} = V_{xr} L / k$ and $p_{yp} = V_{yr} L / k$. Equation (11) can be viewed as the expression of a cosh-Gaussian converted cos-Gaussian beam after having traveled sufficiently along the propagation axis. But this conversion will also occur because of other parameters in question. To this end we introduce I_0 as the ratio of average intensities at two locations on the receiver plane

$$I_0 = < I(p_x = p_{xp}, p_y = p_{yp}, z = L) > / < I(p_x = 0, p_y = 0, z = L) > \qquad (12)$$

Here the average intensities in both the numerator and the denominator are those of Eq. (11). We can then relate the source and link parameters of a cosh-Gaussian converted cos-Gaussian beam to this ratio in the following manner:

$$\frac{\boldsymbol{\rho}_0^4 V_{xr}^2 \boldsymbol{\alpha}_{sx}^2 L^2}{\boldsymbol{\rho}_0^4 L^2 + 4\boldsymbol{\rho}_0^2 \boldsymbol{\alpha}_{sx}^2 L^2 + \boldsymbol{\rho}_0^4 k^2 \boldsymbol{\alpha}_{sx}^4} = 0.5\ell n(2I_0)\,, \quad \frac{\boldsymbol{\rho}_0^4 V_{yr}^2 \boldsymbol{\alpha}_{sy}^2 L^2}{\boldsymbol{\rho}_0^4 L^2 + 4\boldsymbol{\rho}_0^2 \boldsymbol{\alpha}_{sy}^2 L^2 + \boldsymbol{\rho}_0^4 k^2 \boldsymbol{\alpha}_{sy}^4} = 0.5\ell n(2I_0) \qquad (13)$$

4. Results

Although our formulation is applicable to cos-Gaussian beams that can have asymmetrical attributes along the *x* and *y* directions, here we report only the results of symmetrical beams, i.e., $\alpha_{sx} = \alpha_{sy}$ and $V_{xr} = V_{yr}$. When dominant, the existence of a cos term in the cos-Gaussian beam dictates that the intensity will peak at $s_x = 0.5n\pi / V_{xr}$ and $s_y = 0.5n\pi / V_{yr}$, where *n* is an integer starting from zero. Hence we define normalized intensity at the source plane as follows:

$$I_{sN}(s_x, s_y, z = 0) = I_s(s_x, s_y, z = 0) / I_s(s_x = s_y = z = 0) \qquad (14)$$

A three-dimensional view of $I_{sN}(s_x, s_y, z = 0)$ is presented in Fig. 2(a) for a cos-Gaussian beam with typical source parameters. Figure 2(b), on the other hand, displays a contour plot of the same beam. From Fig. 2(a) we note that a cos-Gaussian beam appears as a Gaussian beam modulated with a cos function, where the summits of the successive lobes are aligned in the direction of the slanted axis. Hence for better assessment, the subsequent plots, where the vertical axis refers to intensity distribution, are drawn as side views cut along the slanted axis.

#4763 - $15.00 US Received 7 July 2004; revised 15 August 2004; accepted 13 September 2004

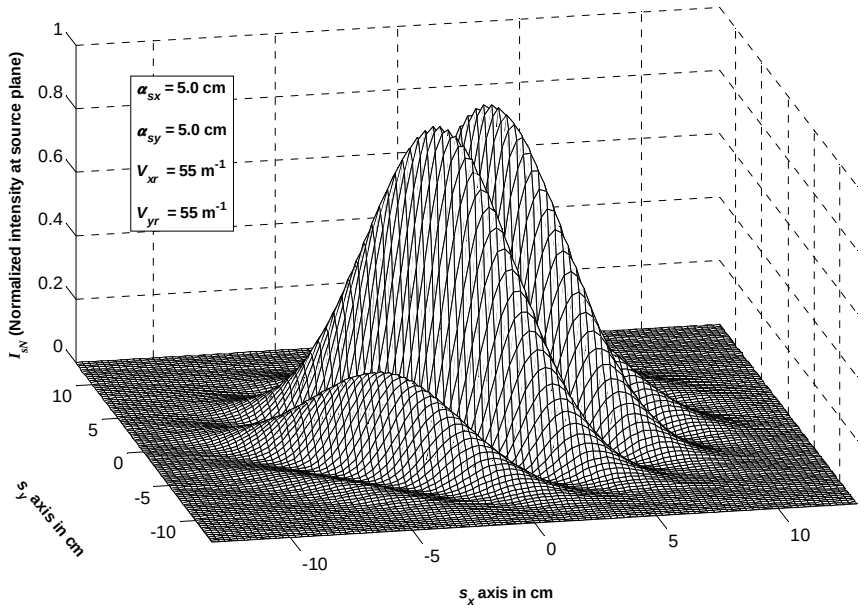

(a)

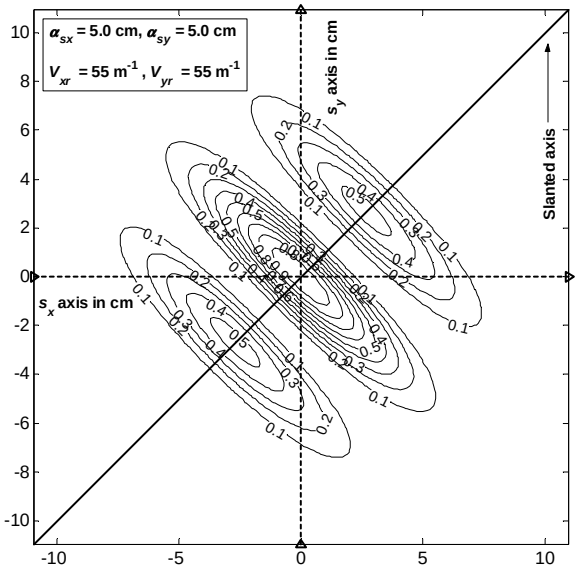

(b)

Fig. 2. (a) Normalized intensity of a cos-Gaussian beam at the source plane and (b) contour plots of the same cos-Gaussian beam.

The normalized average intensity at receiver plane $I_{rN}(p_x, p_y, z = L)$ is defined as

$$I_{rN}(p_x, p_y, z = L) = < I(p_x, p_y, z = L) > / I_s(s_x = s_y = z = 0) \quad (15)$$

#4763 - $15.00 US Received 7 July 2004; revised 15 August 2004; accepted 13 September 2004

The normalized intensity at source plane $I_{sN}(s_x, s_y, z = 0)$ and the normalized average intensity at receiver plane $I_{rN}(p_x, p_y, z = L)$ versus the slanted axis are shown together in Fig. 3(a) for a single cos-Gaussian beam. For cos-Gaussian beam excitation, the beam spreading and the gradual concentration of power within two outer lobes, i.e., the cosh-Gaussian shape, can clearly be identified in Fig. 3(a) for the selected parameters of source size $\alpha_{sx} = \alpha_{sy}$ = 5 cm, link length L = 5 km, wavelength λ = 1.55 μm, the real components of the complex displacement parameters associated with the Gaussian part of the beam in the s_x, s_y directions, $V_{xr} = V_{yr} = 55\,\mathrm{m}^{-1}$, and the structure constant C_n^2 = 1 x 10 $^{-15}$ m$^{-2/3}$. Figure 3(b) shows a contour plot of the same $I_{sN}(s_x, s_y, z = 0)$ and $I_{rN}(p_x, p_y, z = L)$ shown in Fig. 3(a).

For proper investigation of the dependence of average intensity profile on the propagation distance, the real part of complex displacement parameters, turbulence levels, and wavelength of operation, we normalized each profile with respect to its own peak. Normalized average intensity $I_{r0}(p_x, p_y, z = L)$ as defined in this way is

$$I_{r0}(p_x, p_y, z = L) = < I(p_x, p_y, z = L) > / Max\left[< (I(p_x, p_y, z = L) > \right] \tag{16}$$

We note that, after having transformed into a distinct cosh-Gaussian beam, p_x and p_y in the argument of the intensity function in the denominator of Eq. (16) well approximates p_{xp} and p_{yp} derived in Subsection ***3.5.*** Figure 4 displays the variation of $I_{r0}(p_x, p_y, z = L)$ for link lengths L = 0, 2, 10, 20 km. Here the source plane intensity (L = 0) is included and retains the normalization described by Eq. (14). In line with the predictions discussed in Subsection 3.5 and Eq. (11), Fig. 4 confirms, while initially managing to preserve its profile, that the cos-Gaussian beam eventually changes into a cosh-Gaussian beam whose lobe peaks become spaced further apart from the origin in direct proportion to the increasing values of L.

#4763 - $15.00 US Received 7 July 2004; revised 15 August 2004; accepted 13 September 2004

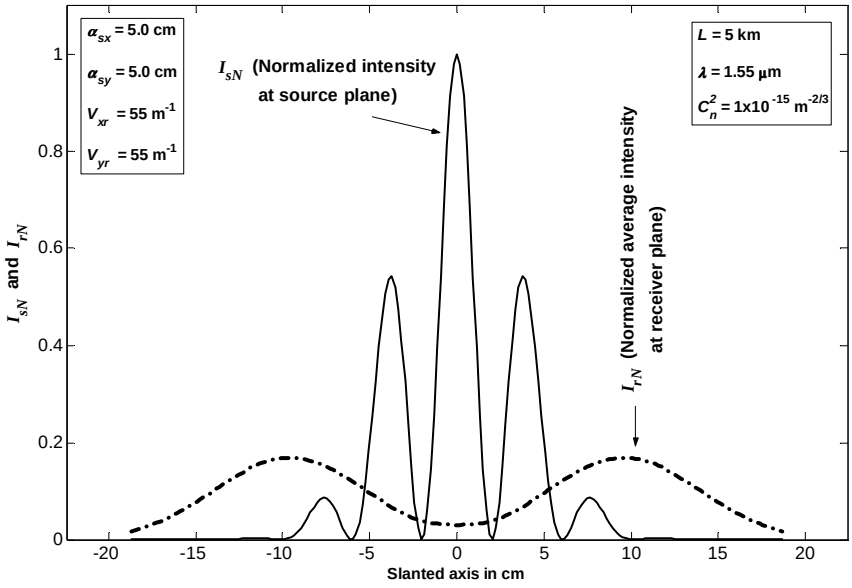

(a)

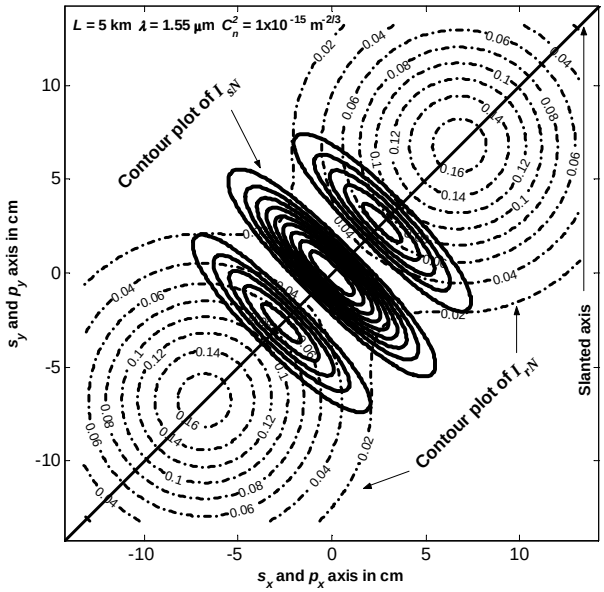

(b)

Fig. 3. (a) Normalized intensity at the source plane and the normalized average intensity at the receiver plane for a typical cos-Gaussian beam and (b) contour plots for the same cos-Gaussian beam.

In Fig. 5 we illustrate the variation of $I_{r0}(p_x, p_y, z = L)$ against the different values of the real components of complex displacement parameters V_{xr} and V_{yr}. Figure 5 demonstrates that

#4763 - $15.00 US Received 7 July 2004; revised 15 August 2004; accepted 13 September 2004

the increases in V_{xr} and V_{yr} serve to accelerate the formation of a cosh-Gaussian beam. This means that for such cases of cos-Gaussian beam excitation, the transformation into a cosh-Gaussian beam occurs at earlier propagation distances.

Figure 6 provides the variation of $I_{r0}(p_x, p_y, z = L)$ at $\lambda = 1.55$ μm and $\lambda = 0.85$ μm in the absence of ($C_n^2 = 0$ m$^{-2/3}$) and in the presence of ($C_n^2 = 1 \times 10^{-14}$ m$^{-2/3}$) turbulence. Here we observe that the presence of turbulence retards the formation of a cosh-Gaussian beam that originates from cos-Gaussian beam excitation. Lowering the wavelength of operation basically has a similar effect.

By considering all the plots in Figs. 4– 6 and Eq. (13), we were able to specify the precise source and propagation conditions that govern the course of conversion from a cos-Gaussian beam into a cosh-Gaussian beam. For example, to accelerate the transformation from a cos-Gaussian beam into a cosh-Gaussian beam, we require

- smaller source sizes α_{sx} and α_{sy},
- larger beam displacement parameters V_{xr} and V_{yr},
- lower structure constants C_n^2,
- higher wavelengths λ,
- longer link lengths L.

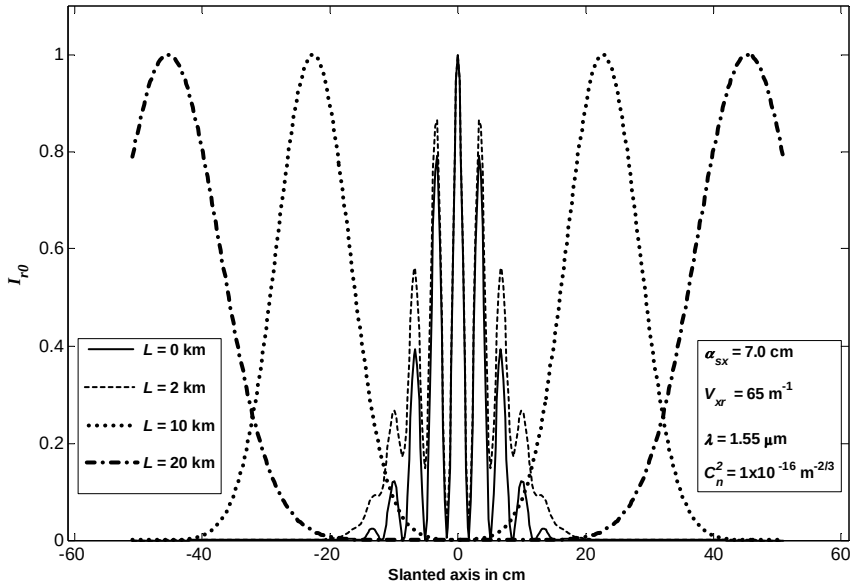

Fig. 4. Dependence of normalized average intensity at the receiver plane on link length.

#4763 - $15.00 US Received 7 July 2004; revised 15 August 2004; accepted 13 September 2004

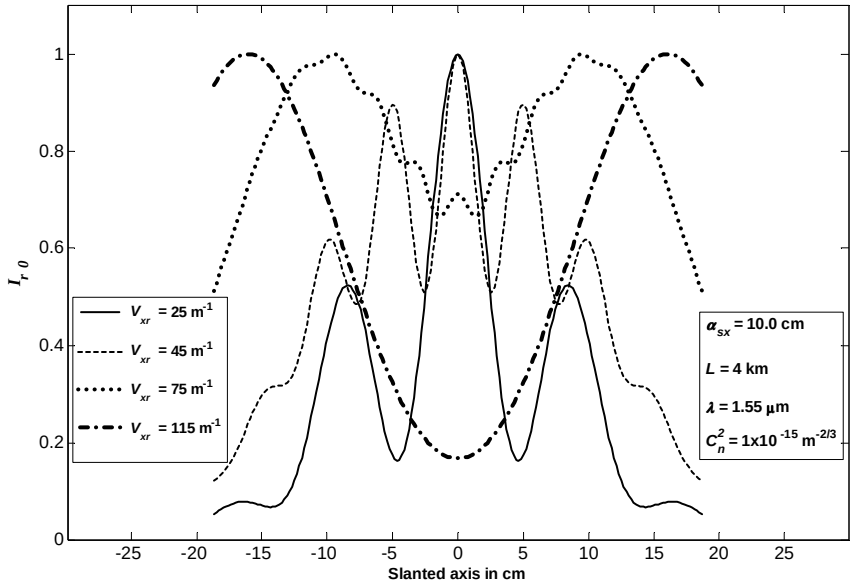

Fig. 5. Dependence of normalized average intensity at the receiver plane on the real part of a complex displacement parameter.

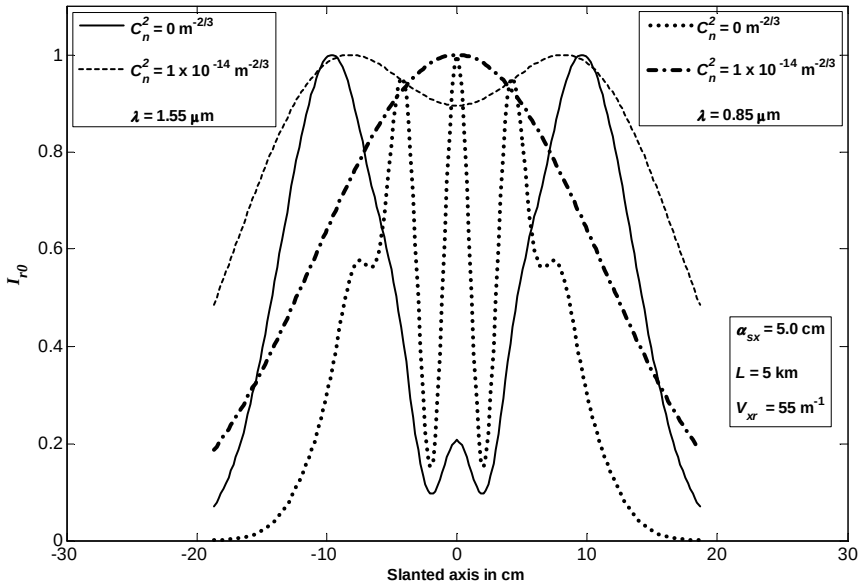

Fig. 6. Dependence of normalized average intensity at the receiver plane on turbulence level and wavelength of operation.

To make comparisons in the reverse direction of reciprocity, i.e., cosh-Gaussian beam changing into a cos-Gaussian beam after propagation in turbulence, we used Eq. (17) from Ref. 16 to provide equivalent graphs of Figs. 4–6 for a cosh-Gaussian source plane excitation. These are Figs. 7–9, where we plotted I_{r0} versus the variations in link length, displacement

#4763 - $15.00 US Received 7 July 2004; revised 15 August 2004; accepted 13 September 2004

parameters, turbulence levels, and wavelengths of operation. In compliance with the findings of Ref. [16], Figs. 7–9 reflect the concrete process of cosh to cos conversion as well as its dependence on link length, displacement parameters, turbulence levels, and wavelengths of operation. Note that a numerically different source and propagation parameters must be used in Figs. 7–9 from those used in Figs. 4–6 to emphasize the conversion from a cosh-Gausssian beam into a cos-Gaussian beam more clearly. From a collective assessment of Figs. 4–9, we can assert that the conversion from a cosh-Gaussian beam to a cos-Gaussian beam runs at a different pace from that of the conversion from a cos-Gaussian beam to a cosh-Gaussian beam. More specifically, the proportionality of factors that accelerate the transformation from a cosh-Gaussian beam into a cos-Gaussian beam is now somewhat modified and can be listed as follows:

- smaller source sizes α_{sx} and α_{sy},
- smaller displacement parameters V_{xr} and V_{yr},
- higher structure constants C_n^2,
- lower wavelengths λ,
- longer link lengths L.

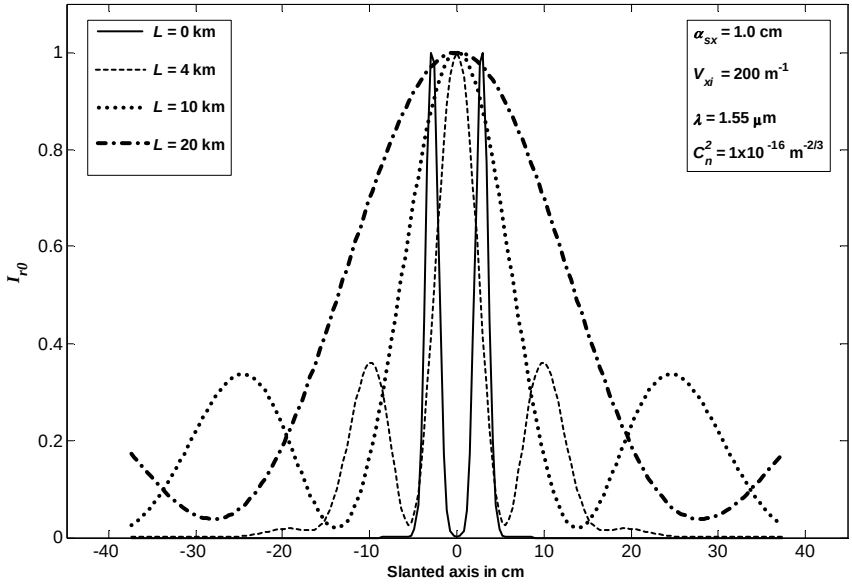

Fig. 7. Dependence of normalized average intensity at the receiver plane on link length (cosh-Gaussian source excitation case).

#4763 - $15.00 US Received 7 July 2004; revised 15 August 2004; accepted 13 September 2004

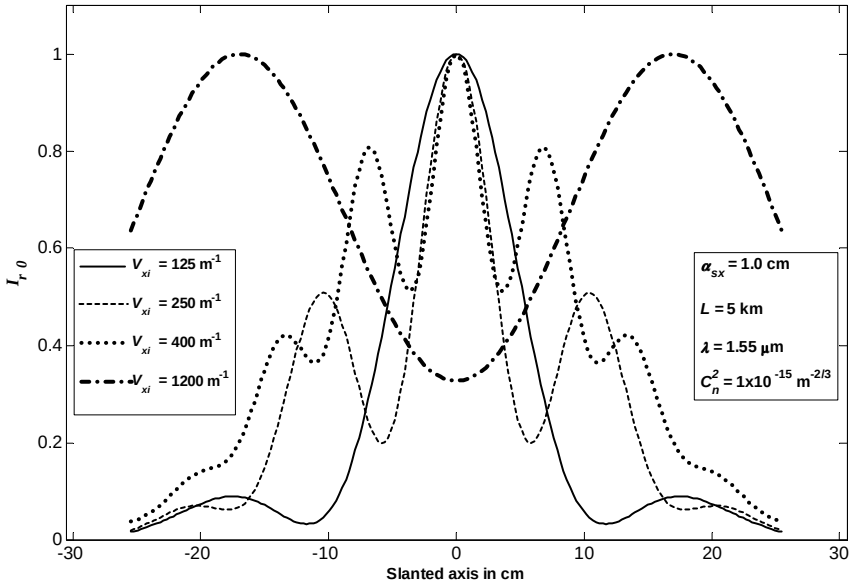

Fig. 8. Dependence of normalized average intensity at the receiver plane on the real part of a complex displacement parameter (cosh-Gaussian source excitation case).

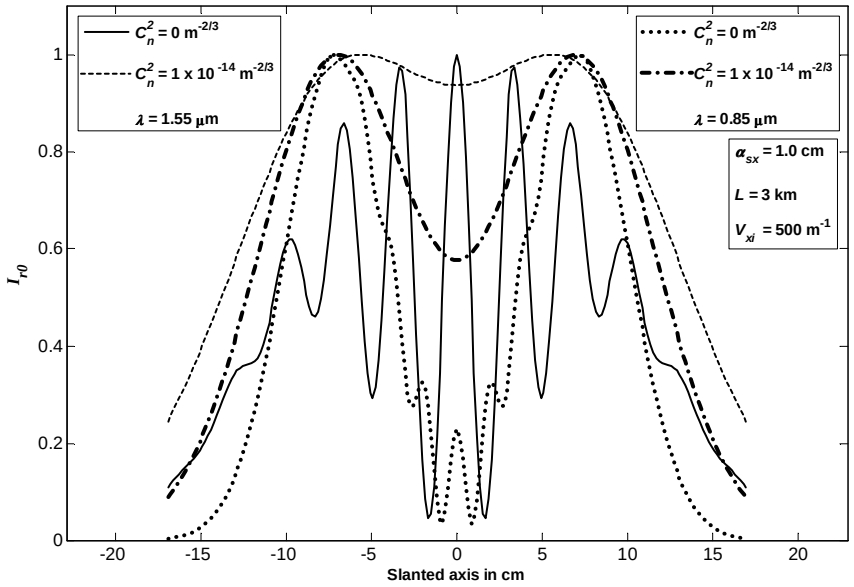

Fig. 9. Dependence of normalized average intensity at the receiver plane on turbulence level and wavelength of operation (cosh-Gaussian source excitation case).

#4763 - $15.00 US Received 7 July 2004; revised 15 August 2004; accepted 13 September 2004

5. Concluding remarks

The average intensity profile of a cos-Gaussian beam in a turbulent atmosphere has been formulated and numerically evaluated. We determined that our average intensity formulation correctly reduces to the existing Gaussian beam wave result in turbulence and the cos-Gaussian beam result in free space (i.e., the absence of turbulence). This formulation further stipulates that a cos-Gaussian beam loses its original shape more rapidly, finally turning into a pure cosh-Gaussian beam with an increase in propagation distance, a real part of the complex displacement parameter and wavelength of operation, and with a decrease in turbulence levels and source sizes. This analytic observation is also supported by the related intensity plots.

Combined with the findings of our earlier research,[16] we assert that cos-Gaussian and cosh-Gaussian beams act in a reciprocal manner in propagation. This means that given the right set of source and propagation parameters, a cos-Gaussian beam at the source plane will lead to a cosh-Gaussian beam at the receiver plane, whereas a cosh-Gaussian source plane beam excitation will arrive as a cos-Gaussian beam at the receiver plane. We refer to this property as the reciprocity of cos-Gaussian and cosh-Gaussian laser beams in a turbulent atmosphere. The same reciprocity phenomenon is also applicable in the absence of turbulence. Transformation from a cos-Gaussian beam into a cosh-Gaussian beam in turbulence is found to accelerate for smaller source sizes, larger beam displacement parameters, lower structure constants, higher wavelengths, and longer link lengths. However, transformation from a cosh-Gaussian beam into a cos-Gaussian beam in turbulence is accelerated for smaller source sizes, smaller beam displacement parameters, higher structure constants, lower wavelengths, and longer link lengths.

Appendix A

Here we give a more extensive explanation of the algebra leading from Eq. (6) to Eq. (7), along with a detailed physical description of the terms that appear in the expression for the averaged intensity profile. Equation (6) contains four separate exponential terms within the braces. These are basically the same terms and differ only in signs of s_{2x}, s_{2y}, V_{xr} and V_{yr}. Hence, once the integration has been performed for one exponential, the rest can simply be obtained by analogy. Moreover we note that there is no coupling between the *x* and the *y* indices, which means that the integrations with respect to s_{1y} and s_{2y} are replicas of the integrations with respect to s_{1x} .and s_{2x}. Consider the first exponential term within braces in Eq. (6) and the integration with respect to s_{1x}, s_{2x} only. By excluding the terms outside the main integral and the terms associated with the s_{1y} and s_{2y} variables, the remainder of the integral in Eq. (6) that we refer to as I_{1x} appears as

$$
\begin{aligned}
I_{1x} = & \int_{-\infty}^{\infty}\int_{-\infty}^{\infty} ds_{1x} ds_{2x} \exp\left[-0.5\left(s_{1x}^2 + s_{2x}^2\right)/\alpha_{sx}^2\right] \exp\left[iV_{xr}\left(s_{1x} + s_{2x}\right)\right] \\
& \times \exp\left[0.5(ik/L)\left(s_{1x}^2 - 2p_x s_{1x} - s_{2x}^2 + 2p_x s_{2x}\right)\right] \exp\left[-\left(s_{1x}^2 - 2s_{1x}s_{2x} + s_{2x}^2\right)/\rho_0^2\right] \\
= & \int_{-\infty}^{\infty} ds_{1x} \exp\left\{\left[-0.5\alpha_{sx}^2 + jk/(2L) - 1/\rho_0^2\right] s_{1x}^2 + \left[iV_{xr} - jkp_x/L + 2s_{2x}\right] s_{1x}\right\} \\
& \times \int_{-\infty}^{\infty} ds_{2x} \exp\left(-0.5 s_{2x}^2/\alpha_{sx}^2\right) \exp\left(iV_{xr} s_{2x}\right) \\
& \times \exp\left[0.5(ik/L)\left(-s_{2x}^2 + 2p_x s_{2x}\right)\right] \exp\left[-\left(s_{2x}^2 + s_{1y}^2 - 2s_{1y}s_{2y} + s_{2y}^2\right)/\rho_0^2\right] \qquad \text{(A1)}
\end{aligned}
$$

#4763 - $15.00 US Received 7 July 2004; revised 15 August 2004; accepted 13 September 2004

The isolated ds_{1x} integral on the third line of Eq. (A1) is in the form of Eq. 3.323.2 of Ref. 18, i.e., in the form of

$$\int_{-\infty}^{\infty} dx \exp\left(-p^2 x^2 \mp qx\right) = \left(\pi^{0.5} / p\right) \exp\left[q^2 / \left(4p^2\right)\right] \tag{A2}$$

After performing the integration over ds_{1x} and the resultant is combined with the other terms inside the ds_{2x}, integral I_{1x} becomes

$$\begin{aligned} I_{1x} = {} & \pi^{0.5} / \left[0.5\alpha_{sx}^2 + 1/\rho_0^2 - jk/(2L)\right]^{0.5} \int_{-\infty}^{\infty} ds_{2x} \\ & \times \exp\left(\left\{0.5\alpha_{sx}^2 + 1/\rho_0^2 + jk/(2L) - \rho_0^{-4} / \left[0.5\alpha_{sx}^2 + 1/\rho_0^2 + jk/(2L)\right]\right\} s_{2x}^2\right) \\ & \times \exp\left(\left\{iV_{xr} + ikp_x / L + \rho_0^{-2}\left(iV_{xr} - ikp_x / L\right) / \left[0.5\alpha_{sx}^2 + 1/\rho_0^2 - jk/(2L)\right]\right\} s_{2x}\right) \end{aligned} \tag{A3}$$

Equation (A3) is again in the form of Eq. (A2). Thus, by similarly performing the integration over ds_{2x} and benefiting from the properties explained in the first paragraph before Eq. (A1) of this Appendix A, we finally arrive at the average intensity at the receiver plane given by Eq. (7), where $\boldsymbol{p} = \left(p_x, p_y\right)$ is the transverse receiver coordinate; k is the wave number; L is the link length; $\rho_0 = \left(0.545\, C_n^2 k^2 L\right)^{-3/5}$ is the coherence length of a spherical wave that propagates in the turbulent medium; C_n^2 is the structure constant; α_{sx} and α_{sy} are the respective source sizes of the Gaussian beam in the s_x and s_y directions; and V_{xr} and V_{yr} denote the real components of V_x and V_y. Here V_x and V_y are the complex displacement parameters along the s_x and s_y directions. $D_{sx} = \left(\rho_0^4 L^2 + 4\rho_0^2 \alpha_{sx}^2 L^2 + \rho_0^4 k^2 \alpha_{sx}^4\right) / \left(\alpha_{sx}^4 L^2\right)$, $D_{sy} = \left(\rho_0^4 L^2 + 4\rho_0^2 \alpha_{sy}^2 L^2 + \rho_0^4 k^2 \alpha_{sy}^4\right) / \left(\alpha_{sy}^4 L^2\right)$ can be interpreted as parameters related to the beam spread in the p_x, p_y directions, respectively.

#4763 - $15.00 US Received 7 July 2004; revised 15 August 2004; accepted 13 September 2004